Evaporation of n-heptane Droplet in a Turbulent Atmosphere at Elevated Pressure and Temperature Conditions – An Experimental Study

Madjid Birouk and Stephen Toth
Department of mechanical and Manufacturing Engineering
University of Manitoba, Winnipeg, Manitoba, Canada

Key words: Droplet, vaporization, turbulence, pressure, temperature

1 Introduction

Spray combustors for power generation operate under turbulent flows at high pressure and temperature conditions. As a result, the mass transport between the ambient gas and liquid phases can be greatly affected. It is well-known that the performance of engineering liquid-fuelled power systems is controlled by the vaporization process of droplets (e.g., [1]). Liquid fuel spray in combustion chambers consists of dense and dilute regions where the dilute spray region may be regarded as an ensemble of isolated single droplets. Therefore, the vaporization and combustion of a single droplet may well be representative of spray's dilute region. This view was supported by recent attempts to construct comprehensive spray combustion numerical codes using research results of isolated droplets (e.g., [2]).

It was recently reported that spray combustion numerical/modeling codes employed by industry rely on untested approximations on the effect of gas phase turbulence on spray gasification [3-4]. This is due to a) the paucity of data and knowledge on the role of gas phase turbulence on droplet gasification especially under realistic test conditions of ambient pressure and temperature [5], and ii) to the belief that turbulence in these systems is controlled by large scales and hence the absence of any interaction between small droplets and these scales. However, recent experiments on the effect of turbulence on the gasification process of fuel droplets, which is still relatively sparse, fuelled the interest in testing and thus including turbulence in the design codes of spray combustion (e.g., [3-4]). Studies on the vaporization of a single droplet in turbulent environment at elevated pressure and temperature conditions are almost inexistent [5]. Early examinations of the vaporization process of a droplet did not include the effect of pressure and temperature. However, recent studies turned more of the attention to the role of pressure on droplet gasification and spray combustion in general. This progress was made possible owing to the theoretical development of more reliable physical expressions capable of determining thermo-physical and transport properties of fluids at high-pressure conditions. A review of recent literature revealed that there exists considerable amount of theoretical/numerical and experimental studies on the gasification process of a droplet exposed to ambient pressure and temperature conditions in the range similar to those encountered in a combustion chamber of liquid-fuelled combustion power systems. On the experimental front, there are only a few studies by, for

Correspondence to: Madjid.Birouk@ad.umanitoba.ca

example, Nomura et al. [6], Ghassemi et al. [7] and Chauveau et al. [8], which reported valuable physical evidence on the role of pressure on the droplet vaporization process. Their findings were important not only for providing physical evidence but also for providing a bank of data for numerical validations. The present work is a continuation of these previous efforts aiming at clarifying the role of turbulence on the gasification process of hydrocarbon fuel droplets. This paper reports new experimental data on the vaporization process of hydrocarbon droplets in a turbulent environment at elevated ambient pressure and temperature conditions.

2 Test Rig and Conditions

The experimental test rig consists mainly of a spherical turbulence chamber/vessel which is made of stainless steel with an inner and an outer diameter of 380 mm and 405 mm, respectively. The apparatus has already been described elsewhere [5]. Therefore, only a brief and complementary description is provided here. Isotropic turbulence is generated by four pairs of opposed axial 6-bladded fans, which are located at a distance of 200 mm across from one another inside the spherical vessel/chamber. The six-bladed fans are each driven by a servomotor. These motors are synchronized and the manual adjustment of the servomotor drive's amplifiers allows for the synchronization of the fans to +/-5 revolutions per minute. The vessel has two pairs of opposed optical/quartz windows. The two pairs are positioned 90 degrees apart. The four quartz windows are designed to enable performing Laser Doppler Velocimetry (LDV) and Particle Image Velocimetry (PIV) velocity measurements, as well as visualization and imaging, under elevated pressure and temperature conditions. The droplet was deposited on the quartz filament and suspended in the center of the vessel/chamber as shown in Figure 1. In order to determine the evaporation rate, the droplet was backlit to enhance the sharpness of the droplet surface. An in-house developed Matlab code was used to determine the droplet size by analyzing the image contrast and defining the droplet surface area. The temporal regression of the projected droplet area was captured using a Nanosence MKIII high speed CCD camera with a resolution of 1280 x 1024 pixels. A shutter speed of 1μs was selected and held constant while the image capture rate was adjusted to take advantage of the camera memory capacity of 815 images. A 3X teleconverter magnifying lens was used in series with a 70-210mm telephoto lens and a 4X magnifying lens filter, the resulting lens magnification gives an effective pixel size of 4.9 μm. This allows the camera to view an area of 6.3 mm x 5 mm in the center of the chamber at a stand-off distance of about 24 cm. The test conditions consisted of turbulence intensity, ambient pressure and temperature of the gas surrounding the droplet, as well as liquid properties (n-heptane was used here). Turbulence is varied by increasing the fans speed from zero up to 6000 rpm. The ambient pressure was varied from 1 atm up to 20 atm, and ambient temperature from room temperature up to 100°C. The droplet initial diameter was in the range of 1 mm.

3 Results

3.1. Turbulence Characterization

Two-component Laser Doppler Velocimetry (TSI 2D-LDV) was used to characterize turbulence within the central region of the chamber/vessel. Because of the size and location of the viewing ports and the spatial requirements of the LDV system, turbulence was characterized only within a 80 mm diameter central volume of the spherical chamber. The airflow was seeded by micro olive oil droplets generated by a LaVision fog generator. A minimum of 40,000 LDV data points were taken for each location along x and y axis to determine the orthogonal mean velocities U and V, and their mean fluctuating components u' and v' at both, atmospheric and elevated, pressure and temperature conditions. Turbulence characterization inside the vessel was presented elsewhere and thus only brief and complementary information is provided here. The results revealed that the mean velocity components were very weak (nearly zero in most cases) and their values are negligible compared with their corresponding fluctuating mean values [5]. The turbulent field generated in the central region of the vessel was found to be nearly isotropic where the level of anisotropy of turbulence is less than 10% within the 40 mm in diameter spherical volume of the vessel, and the isotropy of the turbulent field in the central region of the vessel does not change significantly when the chamber is pressurized from atmospheric pressure up to 20 atm and the temperature is increased up to 100°C. Turbulence inside the chamber was also found to be reasonably homogeneous within a spherical volume of about 40 mm in diameter. Outside of this volume, the non-homogeneity level becomes greater than 10% [5]. An examination of this behaviour revealed that this departure of turbulence homogeneity might be due to the aerodynamics of the fan blades. Figure 2 shows that the relationship between the rotational speed of the fans and the turbulence intensity (i.e., $\sqrt{q}$, m/s, where $q = (u'^2+2v'^2)/2$) is linear. However, turbulence intensity is noticeably higher at flow locations farther away from the center of the vessel (that is closer to the fans) [5]. As mentioned above, the occurrence of higher mean fluctuating turbulence velocity components, which magnifies with an increase in the fans speed, might be caused by the aerodynamics of the fan blades. However, as shown in Figure 2, within the 40 mm in diameter spherical central region, a single relation would suffice to represent the change of turbulence intensity as a function of the fans rotational speed. As can be seen in this figure, the best fit is a linear variation of the turbulence intensity with the fans rotational speed which extends from zero up to 6000 RPM. This linear relation can be expressed as $\sqrt{q}$ (m/s) = 0.00077 N (rpm), where N is the fans rotational speed. This correlation is based on the characterization of turbulence at ambient pressure and temperature in the range of 1 atm – 20 atm, and 20°C – 100°C, respectively.

3.2 Droplet Evaporation

Figure 3 presents the time history of the droplet normalized diameter for different turbulence intensity at a typical ambient pressure (6 bar) and ambient temperature 50°C. It shows clearly that i) the d^2-law is maintained at any condition, and ii) the droplet lifetime shortens as turbulence level increases. Figure 4 shows the droplet averaged vaporization rate as a function of ambient pressure for different fans speed at 50°C. This figure reveals the same trend observed for the case of T_∞ = 25°C [5]. That is, the droplet vaporization rate decreases with ambient pressure for each fans speed. The same figure shows that the droplet vaporization rate is greater at higher turbulence. This can be clearly seen in Figure 5 when normalizing the droplet vaporization rate by the corresponding stagnant/quiescent atmosphere value at the respective ambient pressure. It clearly shows that increasing turbulence level results in a continuous increase in the droplet vaporization rate at a given ambient pressure. The same figure reveals also that the droplet vaporization rate is greater at higher ambient pressure for the same turbulence level. This suggests that the effect of turbulence intensifies with ambient pressure. Figure 6 shows that the droplet vaporization rate versus the ambient pressure for different fans speed at T_∞ = 100°C. This figure shows that the trend of the variation of the droplet vaporization rate with ambient pressure is different than that of the T_∞ = 50°C shown in Figure 4 and T_∞ = 25°C reported in [5]. Two opposed trends can be observed; a decrease of the droplet vaporization rate with ambient pressure in quiescent atmosphere; whereas it increases with ambient pressure in the presence of turbulence around the droplet. This latter behavior has not been observed at lower ambient temperature (T_∞ = 25°C [5] and T_∞ = 50°C in Fig. 4). These observations suggest that there is a strong interplay between turbulence and ambient pressure at relatively elevated ambient temperature. Figure 7, however, reveals similar trends to what was observed at lower temperatures; e.g., at T_∞ = 50°C in Figure 5 and at T_∞ = 25°C in [5]. Finally, Figure 8 shows that the droplet vaporization rate increases with ambient temperature at any given ambient pressure regardless of the flow nature/character around the droplet.

4 Conclusions

Preliminary results showed that the effect of turbulence on the droplet vaporization rate is significant at atmospheric and elevated ambient pressure and temperature conditions. However, the effect of turbulence diminishes as ambient temperature increases. Another interesting finding is that the droplet vaporization rate drops with ambient pressure at ambient temperature lower than 100°C regardless of the level of turbulence. Whereas the droplet evaporation rate increases with ambient pressure in the presence of turbulence around the droplet at 100°C,.

References

[1]. G.M. Faeth, Proc. Combust. Inst. 26 (1996)1593-1612.
[2]. A. Sadiki, M. Chrigui, J. Janicka and M.R. Maneshkarimi, Flow Turbulence and Combust. 75 (2005) 105-130.
[3]. M. Labowsky, D. E. Rosner and M. Arias-Zugasti, Int. J. Heat Mass Transfer, 54 (2011) 2683- 2695.
[4]. D. E. Rosner, M. Arias-Zugasti and M. Labowsky, Chemical Eng. Science, 63(2008) 3909-3922.
[5]. M. Birouk and S. Fabbro, Proc. Combust. Inst. 34(2013) 1577-1584.
[6]. H. Nomura and Y. Ujiie, Proc. Combust. Inst. 26 (1996) 1267-1273.
[7]. H. Ghassemi, S.W. Baek and Q.S. Khan, Combust. Sci. Technol. 178 (2006) 1669-1684.
[8]. C. Chauveau, X., Chesneau and I. Gökalp, Adv. Space Res. 16 (1995) 157-160.
[9]. J. Sato, Studies on droplet evaporation and combustion in high pressures. AIAA Paper 93-0813. 31st Aerospace Sciences Meeting and Exhibit, Reno, Nevada, 1993.

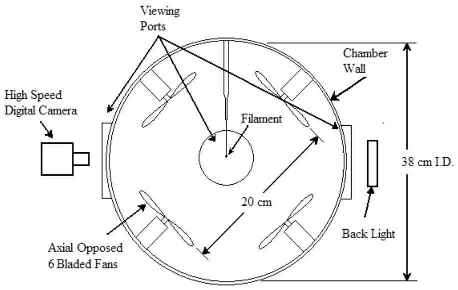

Figure 1. Schematic diagram of the high-pressure spherical vessel/chamber

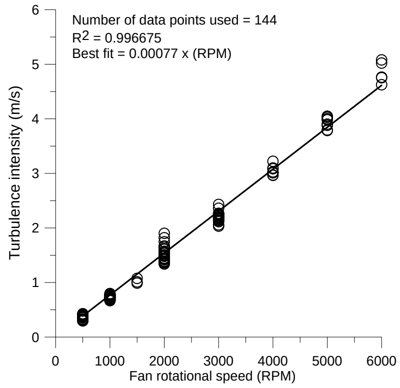

Figure 2. Variation of turbulence intensity, √q (m/s), versus fan rotational speed

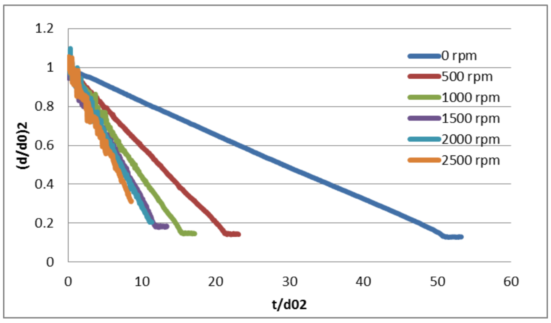

Figure 3. n-heptane droplet time history for different fans speed (turbulence) at a typical ambient pressure (6 bar) and $T_\infty = 50$°C

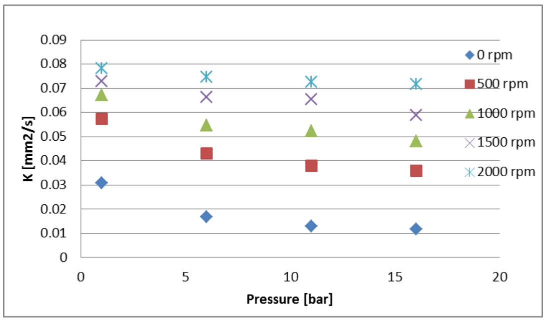

Figure 4. Variation of the vaporization rate of n-heptane droplet with ambient pressure at $T_\infty = 50$°C for different fan speeds (i.e., turbulence intensities)

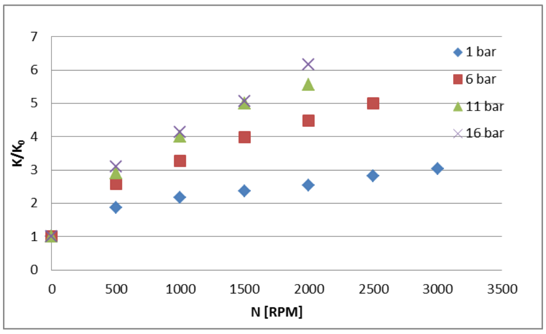

Figure 5. Normalized evaporation rate of n-heptane as a function of fans speed at $T_\infty = 50°C$ for various ambient pressures

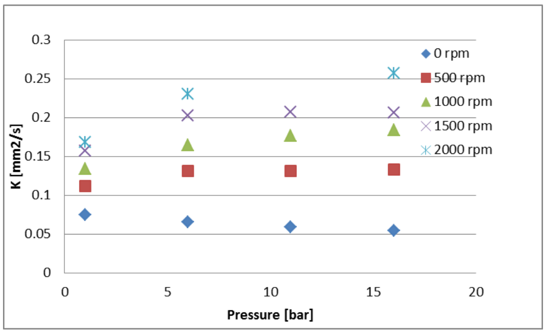

Figure 6. Variation of the vaporization rate n-heptane droplet with ambient pressure at $T_\infty = 100°C$ for different fan speeds (i.e., turbulence intensities)

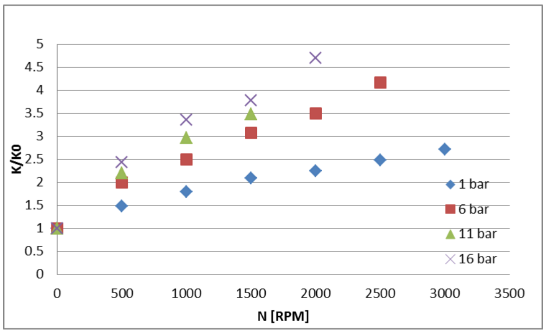

Figure 7. Normalized evaporation rate of n-heptane as a function of fans speed at $T_\infty = 100°C$ for various ambient pressures

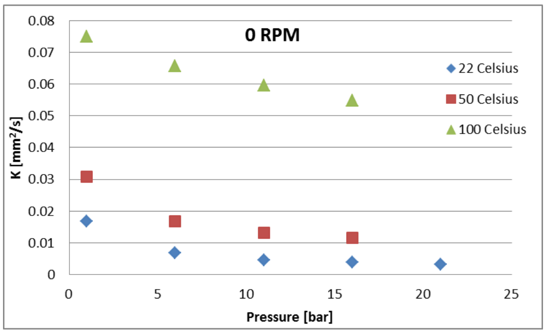

Figure 8. Variation of the vaporization rate of n-heptane droplet with ambient pressure in quiescent environment at different ambient temperatures